Thiadiazoloquinoxaline–Acetylene Containing Polymers as Semiconductors in Ambipolar Field Effect Transistors

ARTICLE *in* JOURNAL OF THE AMERICAN CHEMICAL SOCIETY · AUGUST 2011

Impact Factor: 12.11 · DOI: 10.1021/ja2057709 · Source: PubMed

4 AUTHORS, INCLUDING:

Timea Stelzig
Oerlikon Balzers Surface Solutions
9 PUBLICATIONS **82** CITATIONS
SEE PROFILE

Gunther Brunklaus
University of Münster
79 PUBLICATIONS **1,290** CITATIONS
SEE PROFILE

Martin Baumgarten
Max Planck Institute for Polymer Research
279 PUBLICATIONS **4,309** CITATIONS
SEE PROFILE

JACS
JOURNAL OF THE AMERICAN CHEMICAL SOCIETY

COMMUNICATION

pubs.acs.org/JACS

Thiadiazoloquinoxaline–Acetylene Containing Polymers as Semiconductors in Ambipolar Field Effect Transistors

Timea Dallos, Dirk Beckmann, Gunther Brunklaus, and Martin Baumgarten*

Max Planck Institute for Polymer Research, Ackermannweg 10, 55128 Mainz, Germany

Supporting Information

ABSTRACT: Two conjugated copolymers, PPTQT and PTTQT, were developed based on thiadiazoloquinoxalines connected via ethynylene π-spacer to thiophene units. PPTQT showed maximum hole and electron mobility of 0.028 and 0.042 cm^2/V s, respectively, being the first example of an ambipolar semiconducting material bearing triple bonds in the polymer backbone.

Most of the known organic semiconductors show either high hole or high electron mobility, although the use of a single semiconductor that functions both as p- and n-channel would be highly advantageous.[1−5] Ambipolar semiconductors hold the potential to enable the construction of digital circuits with low power dissipation and high degree of robustness similar to inorganic complementary metal oxide semiconductor (CMOS) logic circuits, while significantly reducing their fabrication complexity.[6−8] Currently, the most successful approach to obtain high mobility ambipolar polymer semiconductors proved to be the alternating donor (D)–acceptor (A) architecture, typically containing thiophene as the electron rich segment.[9] By far, the most studied copolymers in this field are materials based on diketopyrrolopyrrole (DPP) as acceptor.[10,11] More recently, Yang and co-workers showed that by incorporating DPP, benzothiadiazole (BTZ), and thiophene in the same polymer backbone ambipolarity approaching 100% equivalency could be achieved ($\mu_{h,e} \approx 0.1$ cm^2/V s), when applied in field effect transistors (FETs).[12] However, only few materials incorporating other acceptor units have been reported as promising candidates for this application.[9]

Due to their electron deficient nature and good planarity, thiadiazoloquinoxalines (TQ) were incorporated into D–A type polymers and reported as fairly good p-type semiconductors.[13] However, no ambipolar behavior was observed in any of these materials. In all the studied cases, the TQ segment was flanked by two thiophenes and copolymerized with donors such as fluorene ($\mu_h \approx 0.03$ cm^2/V s),[14] thiophene ($\mu_h \approx 3.8 \times 10^{-3}$ cm^2/V s),[15] and dithieno[3,2-b:2′,3′-d]pyrroles ($\mu_h \approx 2.5 \times 10^{-3}$ cm^2/V s).[16] The presence of thiophene units anchoring the TQ core could lead to a torsion angle between the functionalized TQ segment and the neighboring thiophene units, hence decreasing the π-conjugation along the polymer backbone. The incorporation of π-spacers, such as ethynylene, is a feasible option to induce planarity and enhance the π-conjugation along the polymer chain[17] and thus the charge carrier mobility. Furthermore, the oxidation potential might be increased by the presence of electron-withdrawing triple bond spacers.[18] Herein, a series of new copolymers based on functionalized TQ segments (A) connected via ethynylene spacer to alkylated thiophene (D) units for ambipolar FET application is reported. In addition, preliminary studies on the influence of substituents (phenyl vs thienyl) attached to the TQ segment on the corresponding FET performance, microstructure, and morphology are presented as well.

Scheme 1. Synthesis of Thiadiazoloquinoxaline–Acetylene Containing Polymers

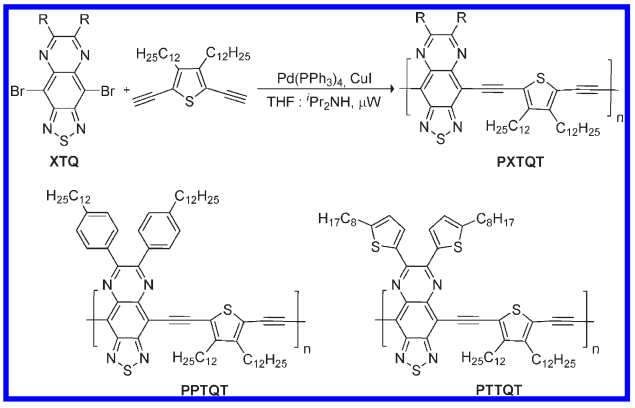

The starting PTQ and TTQ derivatives were synthesized according to our previously reported procedure.[19] The target copolymers were then obtained via microwave-assisted (μW) Sonogashira–Hagihara copolymerization of the corresponding TQ derivative and 2,5-diethynyl-3,4-didodecylthiophene,[20] affording PPTQT and PTTQT, respectively, in rather high yields (>85%, Scheme 1). The full synthetic procedure is described in detail in the Supporting Information. Note that upon purification by Soxhlet extraction with acetone irreversible aggregation occurred. To circumvent this, the studied polymers were not subjected to Soxhlet extraction. Indeed, the presence of alkyl groups along the polymer backbone rendered both copolymers highly soluble in common organic solvents. Based on size exclusion chromatography (SEC) measurements performed in trichlorobenzene solution at 135 °C versus a polystyrene standard, PPTQT and PTTQT presented comparatively high molecular weights of approximately 18 kDA (Table 1; see section S3, Supporting Information). Additionally, both copolymers showed high thermal stability up to 300 °C, with no obvious thermal transition between 20 and 300 °C, respectively.

The optical absorptions of PPTQT and PTTQT in both solution and thin film are illustrated in Figure 1 with the relevant

Received: June 21, 2011
Published: August 11, 2011

Table 1. Optical and Electrochemical Properties of PPTQT and PTTQT

		λ_{max} (nm)/E_g^{opt} (eV)				
polymer	M_n/M_w[a] (kg/mol)	soln[b]	film[c]	E_{HOMO} (eV)[d]	E_{LUMO} (eV)[d]	E_g^{ec} (eV)
PPTQT	18.3/65.2	789	896/1.27	−5.50	−3.96	1.54
PTTQT	17.7/39.1	789	884/1.27	−5.40	−3.91	1.49

[a] SEC in trichlorobenzene at 135 °C vs polystyrene. [b] Dilute toluene solution. [c] Spin-coated from toluene solution (5 mg/mL). [d] HOMO and LUMO levels were estimated from the onsets of the first oxidation and reduction peak, respectively, while the potentials are determined using ferrocene (Fc) as standard.

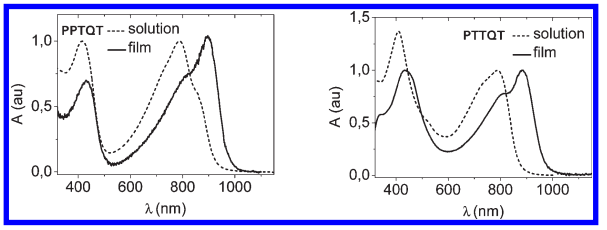

Figure 1. UV−vis absorption spectra of PPTQT (right) and PTTQT (left) in toluene solution and thin film (deposited on a glass substrate by spin-coating a 5 mg/mL toluene solution).

data listed in Table 1. In dilute solution the copolymers revealed an identical long wavelength absorption maximum (λ_{max}). While the shorter wavelength absorption band (350−550 nm) originated from the TQ segments, the band at longer wavelengths (550−950 nm) could be assigned to the D−A interaction through the triple bond spacer. In the solid state, both materials presented a remarkable, over 100 nm red shift of λ_{max}, relative to solution, clearly indicating a greater structural organization in thin film. Furthermore, both compounds retained a shoulder around 800 nm and the short wavelength absorption bands were decreased in intensity with respect to λ_{max}. When compared with PPTQT, the presence of octylthiophene substituents on the TQ core in PTTQT induced a 12 nm blue shift of λ_{max}, without affecting the absorption onset. Notably, the equally low optical band gap of $E_g^{opt} \approx 1.3$ eV indicates rather extensive delocalization of the π-electrons, clearly reflecting the extended π-conjugation and intra- and intermolecular donor (thiophene) acceptor (TQ) interactions.

The HOMO (E_{HOMO}) and LUMO (E_{LUMO}) energy levels were determined from cyclic voltammetry measurements (Table 1; Figure S3.3, Supporting Information). Both copolymers exhibited reversible reductive and irreversible oxidative waves, thus indicating their potential as n-type semiconductors. The electrochemical band gap (E_g^{ec}) is slightly larger (0.2 − 0.3 eV) than E_g^{opt}, which might be attributed to the exciton binding energy of conjugated polymers believed to be in the range of 0.1−0.4 eV.[21] As expected, the E_{HOMO} level of PTTQT (−5.40 eV) was found to be 0.1 eV higher than that of PPTQT (−5.50 eV), as a consequence of the stronger electron donating nature of the thiophene substituents on the TQ segment.

The semiconducting properties were evaluated in bottom contact, bottom gate transistor configuration (Figure 2b). Heavily n-doped silicon was used as gate electrode with a 200 nm thick hexamethyldisilazane (HMDS) treated silicon dioxide layer as

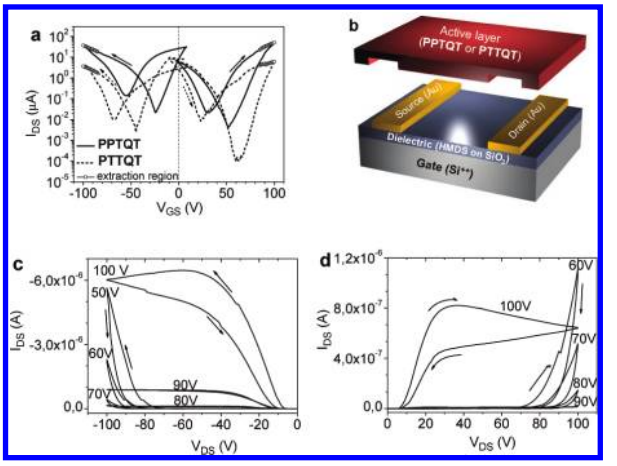

Figure 2. (a) Transfer characteristics of a typical OFET device based on drop-casted PPTQT and PTTQT copolymer from toluene solution. Effective $\mu_h = 0.028$ cm^2/V s and $\mu_e = 0.042$ cm^2/(V s as well as $\mu_h = 1.86 \times 10^{-3}$ cm^2/V s and $\mu_e = 1.62 \times 10^{-3}$ cm^2/V s were obtained for PPTQT and PTTQT, respectively ($L = 20$ μm, $W = 1400$ μm). (b) Schematic representation of the bottom contact, bottom gate transistor structure. (c) p-Channel output characteristics of the FET device having PPTQT as active component with the transfer characteristics presented in (a). (d) n-Channel output characteristics of the FET device having PPTQT as active component with the transfer characteristics presented in (a).

Table 2. FET Performance for PPTQT and PTTQT

	$\mu_{sat,e}$ (cm^2/V s)[a]	$I_{on}/I_{off,e}$ (−)	$\mu_{sat,h}$ (cm^2/V s)[a]	$I_{on}/I_{off,h}$ (−)
PPTQT	0.016 (±0.008)	<10^2	8.7 (±6.6) × 10^{-3}	<10^2
PTTQT	1.1 (±0.3) × 10^{-3}	∼5 × 10^3	1.3 (±0.3) × 10^{-3}	∼4 × 10^2

[a] Average electron and hole mobility obtained from seven measurements with the 90% confidence interval in parentheses.

dielectric. Finally, the semiconducting layer was drop-casted from a 10 mg/mL solution onto the substrates. Different processing solvents were tested, and all prepared devices displayed ambipolar transport characteristics. Nonetheless, the best performance, for both copolymers, was obtained upon deposition from a toluene solution (Table 2). Transistors based on PPTQT revealed the highest hole and electron mobilities of 0.028 and 0.042 cm^2/V s, respectively (calculated from the slope of the $I_d^{1/2}/(V_g)$ curve at $|V_g| = 90 - 100$ V via $I_d = (WC\mu/2L)\cdot(V_g - V_t)$).[22] The typically observed transfer and output characteristics of the transistors are given in Figure 2. Considering that annealing did not improve the FET mobilities for either of the materials, the devices were most optimized on as-casted films. As evidenced in the output characteristics (Figure 2c) at low V_{DS}, the electron transport is injection limited, which possibly originates from the energy offset between the work function of gold and the E_{LUMO} of the active component. Furthermore, the observed hysteresis could be caused by the presence of charge trapping impurities or defects in the polymer such as insufficient interchain packing or domain boundaries with interfacial trap distribution.[23] However, increasing the molecular weights of the polymers or further optimization of either the source or drain electrodes as well as deposition techniques may also lead to improved FET mobilities.[24]

dx.doi.org/10.1021/ja2057709 |J. Am. Chem. Soc. 2011, 133, 13898–13901

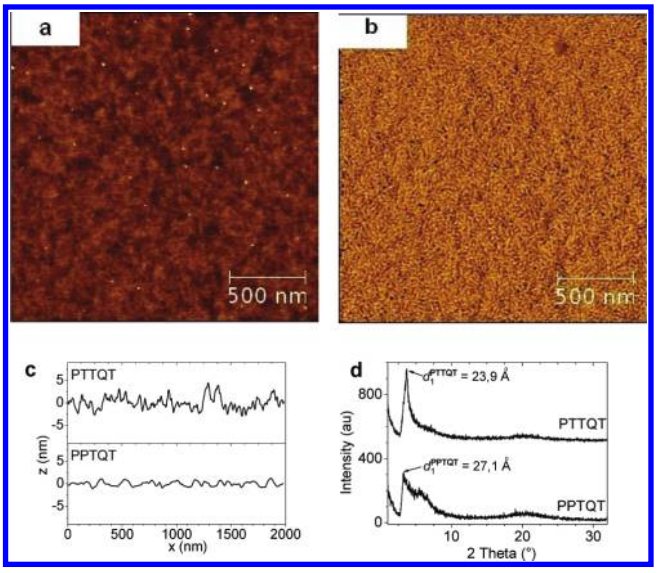

Figure 3. (a, b) AFM topography images of PPTQT (a) and PTTQT (b) thin films inside the transistor's channel. (c) Typical cross section profile of AFM topographic images presented in (a) and (b). (d) $\theta-2\theta$ X-ray diffraction scans of the thin films with the morphological characteristics presented in (a−c).

Notably, due to the employed device architecture, investigation of the microstructure and surface morphology of the active layer via film X-ray diffraction and atomic force microscopy (AFM) (Figure 3; section S4, Supporting Information) was feasible. For both compounds, the X-ray diffraction pattern revealed a highly isotropic organization, showing one first order peak, corresponding to a rather poor 1D lamellar packing perpendicular to the substrate, while no clear indication of $\pi-\pi$ stacking was noticeable. The out-of-plane d_1 spacing was calculated to be 27.1 Å for PPTQT, and a second order peak was extracted as d_2 = 15.4 Å. The AFM image of the same material showed a very smooth (rms roughness of 0.9 nm) amorphous-like superstructure. The d_1 = 23.9 Å spacing corresponding to PTTQT suggests either a tighter lamellar packing or a different tilt angle. Although the larger E_{HOMO} of PTTQT would imply a reduced injection barrier, both the hole and electron mobility proved to be 1 order of magnitude smaller compared to PPTQT. As shown in the corresponding AFM image (Figure 3b), the presence of octylthiophene side chains on the TQ core gave rise to the formation of randomly oriented wormlike morphology with an average length and width of ∼50 and ∼9 nm, respectively (rms roughness of 1.8 nm). This macroscopic organization is more similar to that of *rr*P3HT; therefore, it is reasonable to assume that the lower charge carrier mobility of PTTQT may be due to the domain boundaries created alongside of small worm-like nanofibrills.[25]

Possible packing effects of PPTQT were further studied via solid-state NMR, which provides outstanding selectivity for local environments.[26] While most peaks in the corresponding ^{13}C-CPMAS NMR spectrum were in good agreement with the molecular structure of PPTQT, a set of rather small peaks at 90.9, 88.9, 82.7, and 79.0 ppm, which were attributed to the ethynyl spacers (Figure S3.7, Supporting Information), indicate not only the likely presence of ethynyl end groups but also a minor degree of local $\pi-\pi$-stacking. Notably, the latter cannot be identified from the corresponding ^{1}H−^{1}H DQ MAS NMR spectrum where homonuclear ^{1}H−^{1}H dipolar couplings correlate protons of different chemical entities[27] (Figure S3.8, Supporting Information). The occurrence of a DQ peak at ca. 15 ppm, however, most likely results from so-called DQ relay of aromatic protons with the methyl end groups (at least three-spin coupling), thus suggesting locally disordered alkyl chains and the absence of interdigitation.

In conclusion, we have shown that through the introduction of triple bond π-spacers in the polymeric backbone of a TQ and thiophene containing copolymer resulted in ambipolar field effect behavior with electron and hole mobilities of 0.042 and 0.028 cm^2/V s, respectively. Preliminary investigations showed that the nature of the substituent on the TQ core plays a significant role on the microstructure and surface morphology in thin films, affecting its field effect mobilities. To the best of our knowledge, this is the first example of a triple bond containing polymer presenting ambipolar characteristics, when applied in FETs, reported up to date.

■ ASSOCIATED CONTENT

Supporting Information. Materials and methods, synthesis, characterization, and CV of polymers, FET device preparation, processing solvent and annealing effect on mobilities, and complete ref 10. This material is available free of charge via the Internet at http://pubs.acs.org.

■ AUTHOR INFORMATION

Corresponding Author
martin.baumgarten@mpip-mainz.mpg.de

■ ACKNOWLEDGMENT

Financial support by the European Union within the EC FP7 ONE-P Project 212311 and SolarNtype (MRTN-CT-2006-03553) project is gratefully acknowledged. We also thank Dr. Rüdiger Berger for assistance with the AFM measurements, Michael Steiert for assistance with the XRD measurements, and Dr. Simon Stelzig for fruitful discussions (Max Planck Institute for Polymer Research, Mainz).

■ REFERENCES

(1) Kelley, T. W.; Baude, P. F.; Gerlach, C.; Ender, D. E.; Muyres, D.; Haase, M. A.; Vogel, D. E.; Theiss, S. D. *Chem. Mater.* **2004**, *16*, 4413–4422.
(2) Forrest, S. R. *Nature* **2004**, *428*, 911–918.
(3) Tsao, H. N.; Cho, D. M.; Park, I.; Hansen, M.; Mavrinskiy, A.; Yoon, D. Y.; Graf, R.; Pisula, W.; Spiess, H. W.; Müllen, K. *J. Am. Chem. Soc.* **2011**, *133*, 2605–2612.
(4) Yan, H.; Chen, Z.; Zheng, Y.; Newman, C. E.; Quin, J.; Dötz, F; Kastler, M.; Facchetti, A. *Nature* **2009**, *457*, 679–686.
(5) Meijer, E. J.; De Leeuw, D. M.; Setayesh, S.; van Veenendaal, E.; Huisman, B. H.; Blom, P. W. M.; Hummelen, J. C.; Scherf, U.; Klapwijk, T. M. *Nat. Mater.* **2003**, *2*, 678–682.
(6) Shkunov, M.; Simms, R.; Heeney, M.; Tierney, S.; McCulloch, I. *Adv. Mater.* **2005**, *17*, 2608–2612.
(7) Anthopoulos, T. D.; Setayesh, S.; Smits, E.; Cölle, M.; Cantatore, E.; de Boer, B.; Blom, P. W. M.; de Leeuw, D. M. *Adv. Mater.* **2006**, *18*, 1900–1904.
(8) Roelofs, W. S. C.; Mathijssen, S. G. J.; Bijleveld, J. C.; Raiteri, D.; Geuns, T. C. T.; Kemerink, M.; Cantatore, E.; Janssen, R. A. J.; de Leeuw, D. M. *Appl. Phys. Lett.* **2011**, *98*, 203301.
(9) Facchetti, A. *Chem. Mater.* **2011**, *23*, 733–758.
(10) Bronstein, H.; et al. *J. Am. Chem. Soc.* **2011**, *133*, 3272–3275.

(11) Bijleveld, J. C.; Zoombelt, A. P.; Mathijssen, S. G. J.; Wienk, M. M.; Turbiez, M.; de Leeuw, D. M.; Janssen, R. A. J. *J. Am. Chem. Soc.* **2009**, *131*, 16616–16617.
(12) Cho, S.; Lee, J.; Tong, M.; Seo, J. H.; Yang., C. *Adv. Funct. Mater.* **2011**, *21*, 1910–1916.
(13) Yu, C. Y.; Chen, C. P.; Chan, S. H.; Hwang, G. W.; Ting, C. *Chem. Mater.* **2009**, *21*, 3262–3269.
(14) Chen, M. X.; Crispin, X.; Perzon, E.; Andersson, M. R.; Pullerits, T.; Andersson, M.; Inganäs O. Berggren, M. *Appl. Phys. Lett.* **2005**, *87*, 252105.
(15) Cheng, K.-F.; Chueh, C.-C.; Lin, C.-H.; Chen, W.-C. *J. Polym. Sci., Part A: Polym. Chem.* **2008**, *46*, 6305–6316.
(16) Zhang, X.; Steckler, T. T.; Dasari, R. R.; Ohira, S.; Potscavage, W. J.; Tiwari, S. P.; Coppée, S.; Ellinger, S.; Barlow, S.; Brédas, J.-L.; Kippelen, B.; John R. Reynolds, J. R.; Marder, S. R. *J. Mater. Chem.* **2010**, *20*, 123–134.
(17) Silvetri, F.; Marrochi, A. *Int. J. Mol. Sci.* **2010**, *11*, 1471–1508.
(18) Cremer, J.; Bäuerle, P.; Wienk, M. M.; Janssen, R. A. J. *Chem. Mater.* **2006**, *18*, 5832–5834.
(19) Dallos, T.; Hamburger, M.; Baumgarten, M *Org. Lett.* **2011**, *13*, 1936–1939.
(20) Bäuerle, P.; Pfau, F.; Schlupp, H.; Würthner, F.; Gaudl, K. U.; Balparda Caro, M.; Fischer, P. *J. Chem. Soc., Perkin Trans. 2* **1993**, *3*, 489–494.
(21) Sariciftci, N. S. *Primary Photoexcitations in Conjugated Polymers: Molecular Excitons vs Semiconductor Band Model*; World Scientific: Singapore, 1997.
(22) Katz, H. E.; Huang, J. *Annu. Rev. Mater. Res.* **2009**, *39*, 71–92.
(23) Verlaak, S.; Arkhipov, V.; Heremans, P. *Appl. Phys. Lett.* **2003**, *82*, 745–747.
(24) Tsao, H. N.; Müllen, K. *Chem. Soc. Rev.* **2010**, *39*, 2372–2386.
(25) Zhang, R.; Iovu, M. C.; Jeffries-EL, M.; Sauvé, G.; Cooper, J.; Jia, S.; Tristam-Nagle, S.; Smilgies, D. M.; Lambeth, D. N.; McCullough, R. D.; Kowalewski, T. *J. Am. Chem. Soc.* **2006**, *128*, 3480–3481.
(26) Khan, M.; Brunklaus, G.; Enkelmann, V.; Spiess, H. W. *J. Am. Chem. Soc.* **2008**, *130*, 1741–1748.
(27) Khan, M.; Enkelmann, V.; Brunklaus, G. *J. Am. Chem. Soc.* **2010**, *132*, 5254–5263.